Institute of Theoretical and Experimental Physics

ITEP-30-98

A.Asratyan, M.Balatz, G.Davidenko, A.Dolgolenko,
G.Dzyubenko, A.Evdokimov, A.Gerasimov, V.Kaftanov,
M.Kubantsev, I.Larin, V.Matveev, V.Semyachkin,
V.Verebryusov, and V.Vishnyakov

Search for Neutrino Oscillations in the COSMOS Experiment at Fermilab

M o s c o w 1998

UDK 539.12 M-16

SEARCH FOR NEUTRINO OSCILLATIONS IN THE COSMOS EXPERIMENT AT FERMILAB: Preprint ITEP 30-98/

A.Asratyan,M.Balatz,G.Davidenko,A.Dolgolenko,G.dzyubenko,A.Evdokimov, A.Gerasimov,V.Kaftanov,M.Kubantsev,I.Larin,V.Matveev,V.Semyachkin, V.Verebryusov,V.Vishnyakov - M., 1998 - 20p.

COSMOS is a ν_τ appearance experiment sensitive to very small neutrino-mixing angles and to neutrino mass differences in the cosmologically interesting region. It is desined to demonstrate an unambiguous τ signal, shoud the $\nu_\mu \dashrightarrow \nu_\tau$ transition with a probability that is at least five times larger than the upper limit for a null hypothesis, $P < 1.4 \times 10^{-5}$ at 90% confidence level. By analysing the decayes of charmed particles produced by neutrinos, COSMOS will also provide precision measurements of the CKM matrix element V_{cd} and of the c-quark mass.

В работе приведено описание эксперимента КОСМОС, целью которого является обнаружение ν_τ в интервале очень малых углов смешивания и разностей масс нейтрино в области представляющей большой интерес для космологии. Эксперимент оптимизирован для демонстрации несомненного сигнала от τ лептона, если переход $\nu_\mu \longrightarrow \nu_\tau$ существует с вероятностью по крайней мере в пять раз большей, чем предел для нулевой гипотезы, $P < 1.4 \times 10^{-5}$ на 90% уровне достоверности. Анализ распадов очарованных частиц, рожденных в нейтринных взаимодействиях в эксперименте КОСМОС позволит произвести наиболее точные определения ККМ матричного элемента V_{cd} и массы с-кварка.

Fig. - 9, ref. - 24 name.

---

1 ITEP group of E803/COSMOS Collaboration

1 Introduction

Whether or not the leptonic number is violated, or alternatively, whether or not the three known lepton generations are independent, is still an important open problem of particle physics. The leptonic number may be violated, if the current neutrinos ν_α ($\alpha = e,\ \mu,\ \tau$) are not exactly massless, but rather represent linear combinations of the mass eigenstates ν_i ($i = 1,\ 2,\ 3$): $\nu_\alpha = U_{\alpha i}\nu_i$, where $U_{\alpha i}$ is a unitary mixing matrix that is analogous to the Cabibbo-Kobayashi-Maskawa matrix for the quark sector. Then, as different mass components no longer propagate coherently, one current neutrino may oscillate in flight to another current neutrino [1]: $\nu_\alpha \rightarrow \nu_\beta$, $\alpha \neq \beta$. For the case of mixing between just two mass eigenstates with masses m_1 and m_2, the corresponding current neutrinos oscillate in space with a wavelength of $\lambda = 4\pi E_\nu \hbar c/\delta m^2$, where $\delta m^2 = m_1^2 - m_2^2$. Note that for $E_\nu = 1$ MeV and $\delta m^2 = 1$ eV^2, the wavelength of the flavor-changing transition reaches a macroscopic value of 2.4 m that is measurable.

Over a distance L from the point of emission, one current neutrino may transform into another with a probability

$$P(\alpha \rightarrow \beta) = \sin^2(2\theta)\sin^2(\pi L/\lambda),$$

where θ is the mixing angle. At distances $L << \lambda$, the transition probability is seen to be proportional to $(L\delta m^2/E_\nu)^2$. Therefore, sensitivity to the lowest values of δm^2 may in principle be improved by pushing down the mean energy of the neutrino, $\langle E_\nu \rangle$, and by increasing the distance L between the source of neutrinos and the detector.

In experimental searches for neutrino oscillations, two different approaches (or a combination of both) are used. In "disappearance" experiments dealing with a single neutrino flavor ν_α, one derives the probability $P(\alpha \rightarrow \alpha)$ by comparing the observed and predicted fluxes of ν_α at the detector position. Then, the quantity $1 - P(\alpha \rightarrow \alpha)$ may be interpreted as the probability for ν_α to oscillate to any other flavor, including exotic flavors like sterilee neutrinos. (The typical examples are the experiments with solar and reactor neutrinos, where the energy of initial electron (anti)neutrinos is below threshold for producing either muons or τ leptons.) Alternatively, in the "appearance" mode one directly measures the probability of a flavor-changing transition, $P(\alpha \rightarrow \beta)$, by detecting the charged-current interactions of the ν_β in a beam initially composed of ν_α neutrinos. For this, the energy of the neutrino beam must be well above the threshold for production of the charged lepton, l_β. Most accelerator experiments rely on the appearance technique.

Searches for neutrino oscillations are actively pursued in experiments with solar, atmospheric, reactor, and accelerator neutrinos. These are characterized by very different L/E_ν ratios and, therefore, are sensitive to very different values of Δm^2. Measurements of the ν_e flux from the Sun [2] fall short of predictions of the solar model. The claimed large deficit of solar neutrinos suggests a $\nu_e \to \nu_X$ transition with δm^2 in the range of either 10^{-10}–10^{-11} eV^2 (for the vacuum solution) or 10^{-4}–10^{-5} eV^2 (for the matter-enhanced oscillations, see [3]). The lower-than-expected ν_μ/ν_e ratio for atmospheric neutrinos [4] suggests either the $\nu_\mu \to \nu_e$ or $\nu_\mu \to \nu_\tau$ transitions with δm^2 on the order of 10^{-2}–10^{-3} eV^2 and with a large mixing. An accelerator experiment using neutrinos from π^+ and μ^+ decays at rest [5] has presented evidence for the $\bar{\nu}_\mu \to \bar{\nu}_e$ transition with $\delta m^2 > 1$ eV^2. At the same time, the accepted scheme with three neutrino flavors allows only two mass scales for δm^2. The situation should be clarified by the currently running and forthcoming experiments.

In analogy with the known pattern of quark mixings, one may naively expect that mixings between the neighboring neutrino flavors (*i.e.*, ν_e–ν_μ and ν_μ–ν_τ) should be the strongest, while that for ν_e–ν_τ may be substantially weaker. Qualitatively, one might expect that the mass hierarchy of neutrinos follows that of corresponding charged leptons, so that ν_τ should be the most massive. Indeed, the GUT see-saw mechanism [6] predicts that $m_{\nu_e}/m_{\nu_\mu}/m_{\nu_\tau} \sim m_u^2/m_c^2/m_t^2$. Thus, the transition $\nu_\mu \to \nu_\tau$ may have the largest mixing and the largest value of δm^2, and therefore could be the most promising for experimental investigation. At the same time, the transition $\nu_\mu \to \nu_\tau$ can be efficiently probed at accelerators that offer intense and almost pure beams of muon neutrinos with mean energy in excess of the threshold for τ production, as required by an experiment with ν_τ appearance.

The flux of τ neutrinos generated via the flavor-changing transition $\nu_\mu \to \nu_\tau$ can only be inferred from the number of τ leptons produced in the charged-current reaction $\nu_\tau N \to \tau^- X$. The created τ typically travels a distance of a few hundred microns in space (lifetime 3×10^{-13} s) and then decays either leptonically with emission of two neutrinos ($\tau^- \to \mu^- \bar{\nu}\nu$, $e^- \bar{\nu}\nu$) or hadronically with emission of a single neutrino ($\tau^- \to \pi^- \nu$, $\rho^- \nu$, $a_1^- \nu$, *etc.*). An efficient search for the $\nu_\mu \to \nu_\tau$ transition requires that the events of τ production and decay be selected and analyzed on an event-by-event basis. Therefore, the production and decay vertices must be reliably resolved in the detector (whereby the short track of the τ is reconstructed in space) and the decay particles must be selected. Of the available detector choices, only nuclear emulsion fully meets the above requirements for a massive target.

Indeed, it was the emulsion technique that was employed by the Fermilab experiment E531 in a search for the $\nu_\mu \to \nu_\tau$ transition [7] that resulted in zero candidate events of τ production and decay. The corresponding exclusion plot in the $\sin^2(2\theta)$–δm^2 plane is illustrated in Fig. 1. For $\delta m^2 > 50$ eV^2, the mixing parameter $\sin^2(2\theta)$ was restricted to be less than 5×10^{-3}. Of the subsequent $\nu_\mu \to \nu_\tau$ experiments, the emulsion technique was employed by CHORUS at CERN SPS [8]. This experiment completed data taking in 1997, though data processing is still in progress. Provided that no candidate events are finally seen, they will tighten the E531 upper limit on $\sin^2(2\theta)$ by another order of magnitude, see Fig. 1.

In this paper, we discuss the design and physics potential for $\nu_\mu \to \nu_\tau$ of a next-generation experiment, E803/COSMOS at Fermilab [9, 10]. The detector will operate in the intense neutrino beam of the Main Injector – a 120-GeV proton accelerator under construction at Fermilab. (As far as 735 km downstream, the same beam will service a long-baseline neutrino experiment, MINOS [11].) The startup of the experiment is scheduled for the year 2000.

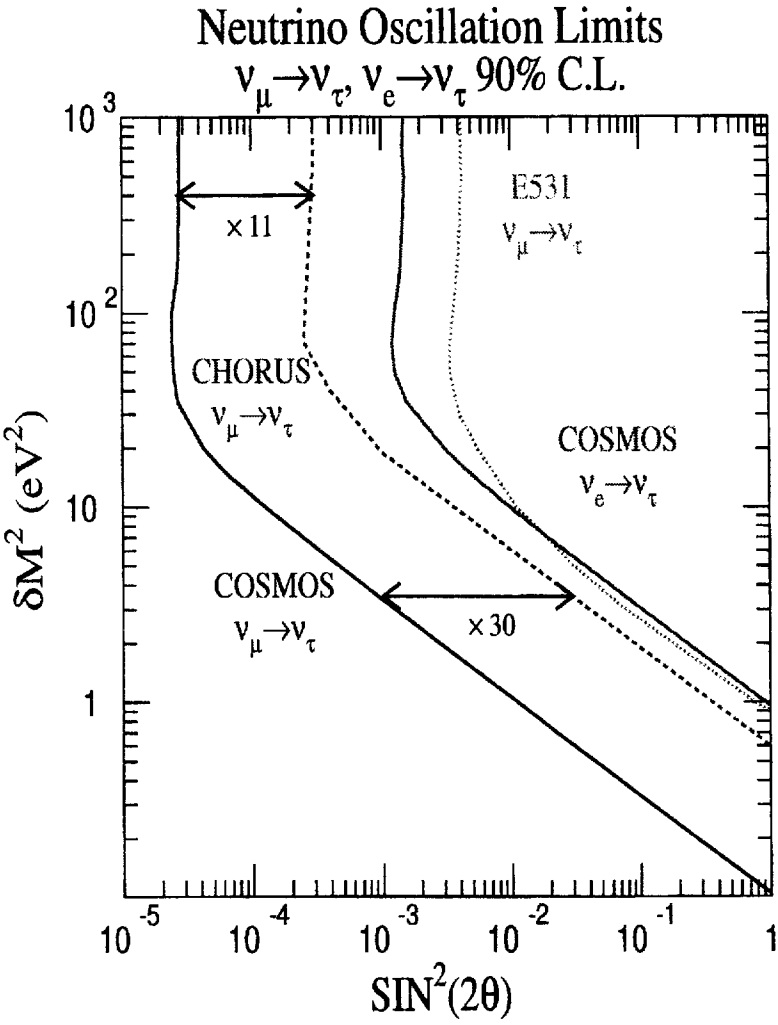

Figure 1: Comparison of the projected exclusion plots of E803/COSMOS and CHORUS for the null hypothesis (90% CL), and the existing limit of the E531 experiment. Note that E803/COSMOS is approximately 30 times more sensitive than CHORUS for low values of δm^2. Furthermore, the COSMOS limit for $\nu_e \rightarrow \nu_\tau$ is four times better than the E531 limit for $\nu_\mu \rightarrow \nu_\tau$.

2 Discovery Potential of E803/COSMOS

Like CHORUS at CERN, COSMOS is designed as a hybrid detector combining an emulsion target with a downstream electronic spectrometer. The candidates for τ decays are directly observed in the emulsion target, while the spectrometer is used to select the events to be scanned in emulsion and to measure the momenta of secondary particles for kinematic analysis of τ candidates. The emphasis is made on identifying the one-prong decays

$$\tau^- \to \pi^- \nu \ (BR = 11.3\%),$$
$$\tau^- \to \rho^- \nu, \quad \rho^- \to \pi^- \pi^0 \ (BR = 25.2\%),$$
$$\tau^- \to e^- \bar{\nu} \nu \ (BR = 17.8\%),$$

as well as

$$\tau^- \to \mu^- \bar{\nu} \nu \ (BR = 17.4\%).$$

Note that in the original E803/COSMOS proposal [9], the analysis of the muonic mode was not foreseen because of the considerable scan load from ν_μ-induced CC interactions. Owing to recent advances in the technique of automatic scanning, the analysis of this mode becomes possible. The three-prong decays of the τ, that have very distinctive signatures in emulsion and a net branching fraction of 15%, are plagued by the background from three-prong interactions of hadrons like pion dissociation on nuclei. Whether or not the three-prong decays of the τ can finally be separated from background using decay kinematics is under investigation.

As any next-generation experiment, COSMOS must boast a higher sensitivity to the $\nu_\mu \to \nu_\tau$ transition than CHORUS. Some characteristics of the two experiments are compared in Table 1.

The competitive edge of COSMOS as a robust next-generation experiment rests on (i) a large sample of neutrino interactions to be collected, and (ii) a capability to reliably identify and reconstruct τ decays in a number of channels.

2.1 Statistics and the Null Limit

Owing to a higher repetition rate and more protons per spill compared to the SPS accelerator at CERN (see Table 1), the Main Injector will deliver to primary target 30 times more protons per year. As a result, COSMOS will eventually collect 16 times more ν_μ-induced CC events than CHORUS, and therefore must reject the background to τ decays much more efficiently. Indeed, in COSMOS the number of background events per ν_μ-induced CC interaction is expected to be 20 times less than in CHORUS.

Even though the lower neutrino energy of COSMOS implies a stronger threshold suppression of τ production, much higher statistics of neutrino events will permit a tighter restriction on the $\nu_\mu \to \nu_\tau$ transition if no signal is observed (the null limit at 90% CL), see Fig. 1. In the null limit, the projected sensitivity of COSMOS is seen to be 10 times better for $\delta m^2 > 50$ eV^2, and 30 times better for low values of dm^2 that are the most interesting from the viewpoint of cosmology. Suppose CHORUS just misses a true τ signal that is equal to their upper estimate of total background at 90% CL, 3.8 events. Then, COSMOS with detect some 40 events for $\delta m^2 > 50$ eV^2, and as many as 120 events if $\delta m^2 < 30$ eV^2.

Quantity Compared	COSMOS	CHORUS
Proton energy, GeV	120	450
Protons per cycle	$4 \cdot 10^{13}$	$2 \cdot 10^{13}$
Cycle time, s	1.9	14.4
Protons per year	$3.7 \cdot 10^{20}$	$1.2 \cdot 10^{19}$
Length of decay channel, m	800	414
Distance from target to detector, m	960	806
$\langle E \rangle$ of ν_μ beam (by flux), GeV	12	27
$\langle E \rangle$ of ν_μ-induced CC events, GeV	18	39
$\langle E \rangle$ of ν_τ-induced CC events, GeV	24	54
$\langle L/E \rangle$, km/GeV	0.023	0.011
$\langle \sigma(\nu_\tau) \rangle / \langle \sigma(\nu_\mu) \rangle$	0.27	0.51
Background per ν_μ-induced CC event	$1.7 \cdot 10^{-7}$	$3.4 \cdot 10^{-6}$
Trigger, fiducial, and scan efficiency	0.73	0.61
Σ (BR $\times$ efficiency)	0.114	0.097
Total number of ν_μ-induced CC events	$8.1 \cdot 10^6$	$5.0 \cdot 10^5$
Total number of background events	1.3	1.7
Total background events, 90% CL	3.5	3.8
Reach in $\sin^2(2\theta)$ for large δm^2	$2.8 \cdot 10^{-5}$	$3.1 \cdot 10^{-4}$
Reach in δm^2 for maximum mixing, eV^2	0.10	0.58

Table 1: Comparison of some parameters of the COSMOS and CHORUS experiments. The data on CHORUS come from their updated proposal of 1993 [8].

2.2 Identifying and Reconstructing τ Decays in Emulsion

That the experiment be capable of convincingly interpreting and demonstrating even a relatively small τ signal, should one show up, is perhaps much more important than just restricting the parameter space for a null-limit hypothesis. COSMOS is designed to demonstrate an unambiguous τ signal in several decay channels, once the actual probability of the $\nu_\mu \to \nu_\tau$ transition is at least five times larger than the quoted upper limit (at 90% CL) for the null hypothesis. The ability of COSMOS to identify, in particular, the (quasi)-two-particle decays like $\tau^- \to \pi^-\nu$ and $\tau^- \to \rho^-\nu$, $\rho^- \to \pi^-\pi^0$ is based on advanced spectrometry for charged particles and photons, as well as on measuring the direction of the τ track in emulsion to better than 1 mrad.

In a two-body decay of a massive particle, the "transverse mass" is defined as $M_T = (p_T^2 + m_1^2)^{1/2} + (p_T^2 + m_2^2)^{1/2}$, where m_1 and m_2 are masses of the daughters and p_T is their transverse momentum with respect to parent direction. Kinematically, M_T should show a peak near the mass of the parent; the width of the peak critically depends on experimental resolutions in parent direction and in 3-momenta of the daughters. The transverse-mass distributions for the $\pi^-\nu$ and $\rho^-\nu$ decays, smeared with the experimental resolutions of COSMOS, are illustrated in Fig. 2. Despite the smearings, these still reveal the characteristic Jacobian cusps near the endpoint. In CHORUS, the sharp edge of the M_T distribution is completely destroyed by the inferior resolutions for secondary particles that are momentum-analyzed after crossing the coils of the spectrometer magnet, where they may interact or suffer Coulomb scatterings.

The M_T technique for identifying massive parents by two-body decays in emulsion has been proven by observing the decays $D_s^+(1968) \to \mu^+\nu$ [12] against a heavy background from other

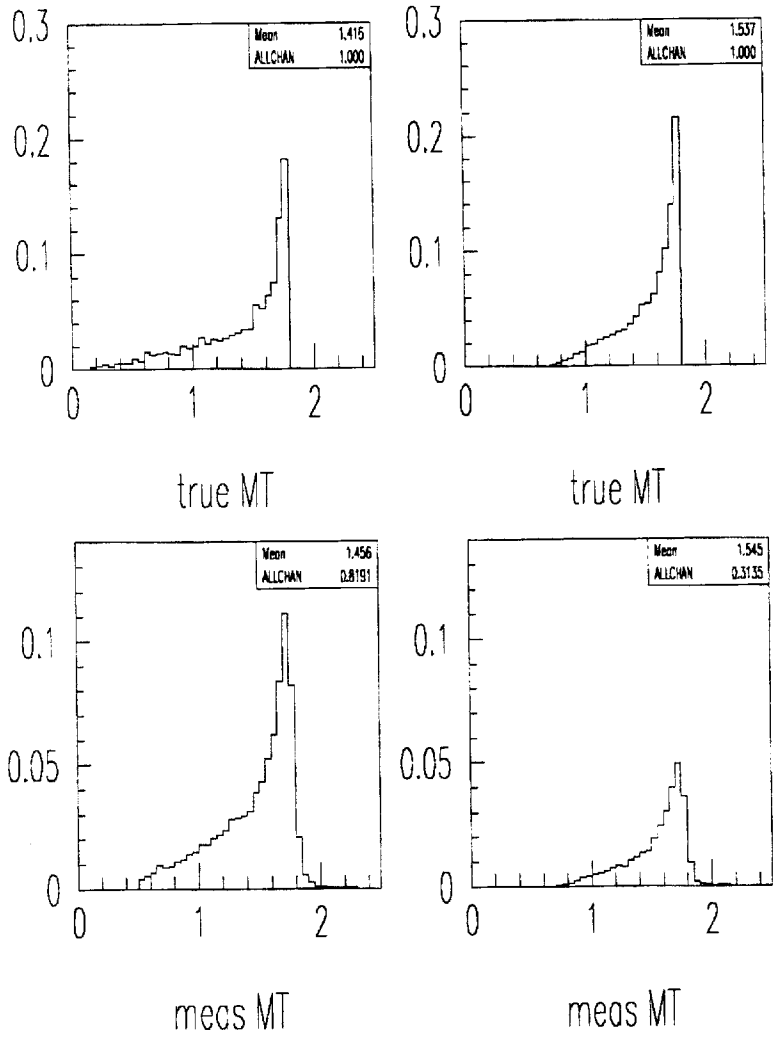

Figure 2: Transverse mass $M_T = \sqrt{p_T^2 + m_h^2} + p_T$ for the (quasi-)two-body decays $\tau^- \to h^-\nu$ with $h^- = \pi^-$ (left-hand column) and $h^- = \rho^- \to \pi^-\pi^0$ (right-hand column). The unsmeared and smeared M_T distributions are shown in the top and bottom rows, respectively.

decays of charm. That the transverse mass peaks near the true mass was also exploited in measurements of the W mass in collider experiments [13].

Yet another kinematic handle involves analyzing the production-decay process $\nu_\tau N \to \tau^- X$, $\tau^- \to \nu h^-$ (where h^- is either π^- or ρ^-) as a whole. Let $\Phi_{\tau X}$ be the azimuthal angle between the τ and primary hadrons' 3-momenta with respect to the incident-neutrino direction, and $\Phi_{\nu h}$ be the azimuthal angle between the decay neutrino and the decay hadron h with respect to τ direction. Ideally, in either case the two objects are emitted back-to-back, so that one would expect that $\Phi_{\tau X} = 180^0$ and $\Phi_{\nu h} = 180^0$. Actually, the former azimuth is distorted by uncertainties on the τ and primary hadrons' directions, while the latter azimuth requires knowledge of the p_T vector of the undetected neutrino from τ decay, that can only be estimated as missing p_T of the event as a whole. That the measured values of both azimuthal angles be close to 180^0 is a challenging requirement on the spectrometer. The simulated two-dimensional distributions in $\Phi_{\tau X}$ and $\Phi_{\nu h}$ for the $\pi^-\nu$ and $\rho^-\nu$ decays of produced τ leptons, smeared with the experimental resolutions of COSMOS, are illustrated in Fig. 3. That both distributions still peak at $\Phi_{\tau X} = 180^0$ and $\Phi_{\nu h} = 180^0$ further demonstrates the capability of COSMOS to reliably select and identify the (quasi)-two-particle semileptonic decays of the τ.

3 Neutrino Beam and Detector

COSMOS will operate in a wideband neutrino beam with double-horn focusing from the Tevatron Main Injector (proton energy 120 GeV). The detector will be placed 160 m downstream of the end of the 800-m-long decay pipe of 1-m radius. The simulated energy spectra for charged-current events induced by different components of the neutrino beam (ν_μ, ν_e, $\bar{\nu}_\mu$, and $\bar{\nu}_e$) are shown in Fig. 4.

Apart from high intensity, a merit of the discussed beam that is crucial for COSMOS is low contamination by antineutrinos for $E_\nu > 8$ GeV : anticharm production by antineutrinos is one of the major sources of background to the τ signal (see below). The present beam will generate nearly 140 times less $\bar{\nu}_\mu$-induced than ν_μ-induced charged-current interactions. Originally, a shorter decay pipe of 320 m was envisaged [9]; increasing its length to the presently adopted value of 800 m results in a better sensitivity to small values of δm^2 that are cosmologically interesting, while slightly reducing the sensitivity for $\delta m^2 > 50$ eV^2.

The elevation view of the COSMOS spectrometer is presented in 5. Its major subsystems are the emulsion target, the tracker for charged particles, the spectrometer magnet, the electromagnetic calorimeter, and the muon identifier. COSMOS is quite different from conventional neutrino detectors that usually consist of many identical modules. A hybrid spectrometer is an organic whole which cannot be staged: all subsystems of the detector play interrelated roles in locating and reconstructing events. The major issues of the detector design are:

1. Large mass of the emulsion target for increased sensitivity. Target area is largely limited by the transverse dimensions of the beam and by the size of the downstream calorimeter, while target thickness is limited by showering and secondary interactions. The emulsion target has a thickness of 3 radiation lengths, and thus most events will contain well-developed electromagnetic showers that complicate tracking near the emulsion. These showers must be "reassembled" to kinematically reconstruct the events.

2. Ability to link tracks between the spectrometer and the emulsion. This implies efficient tracking in the high-multiplicity environment resulting from the thick target, good reso-

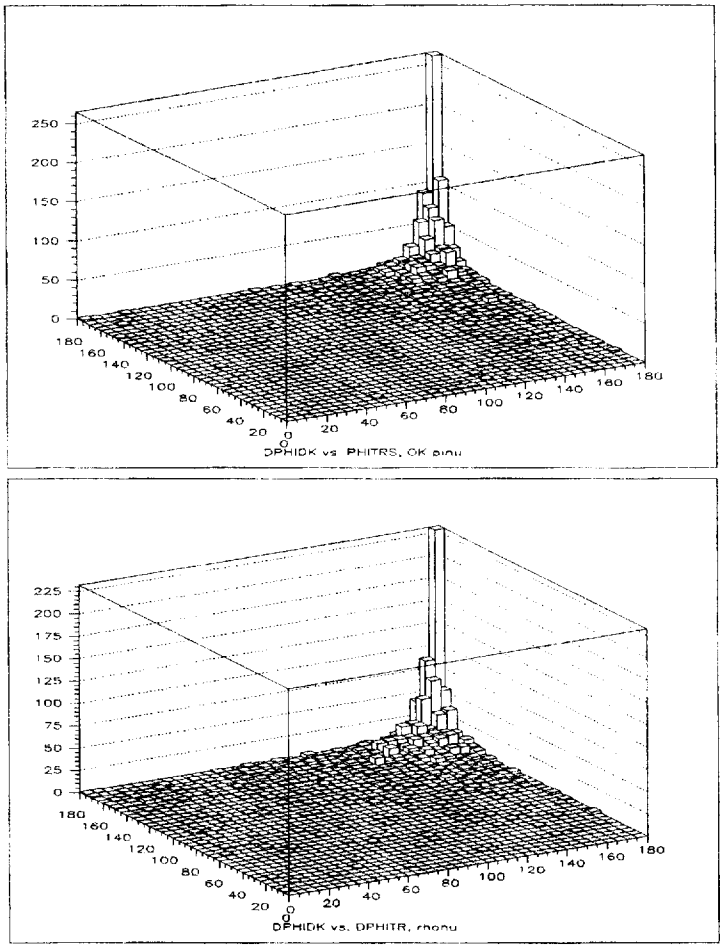

Figure 3: The simulated two-dimensional distributions in the azimuthal angles $\Phi_{\tau X}$ and $\Phi_{\nu h}$ (see text) for the $\pi^-\nu$ (top) and $\rho^-\nu$ (bottom) decays of produced τ leptons, smeared with the experimental resolutions of COSMOS. That both distributions still peak at $\Phi_{\tau X} = 180^0$ and $\Phi_{\nu h} = 180^0$ further demonstrates the capability of COSMOS to reliably select and identify the semileptonic (quasi)-two-particle decays of the τ.

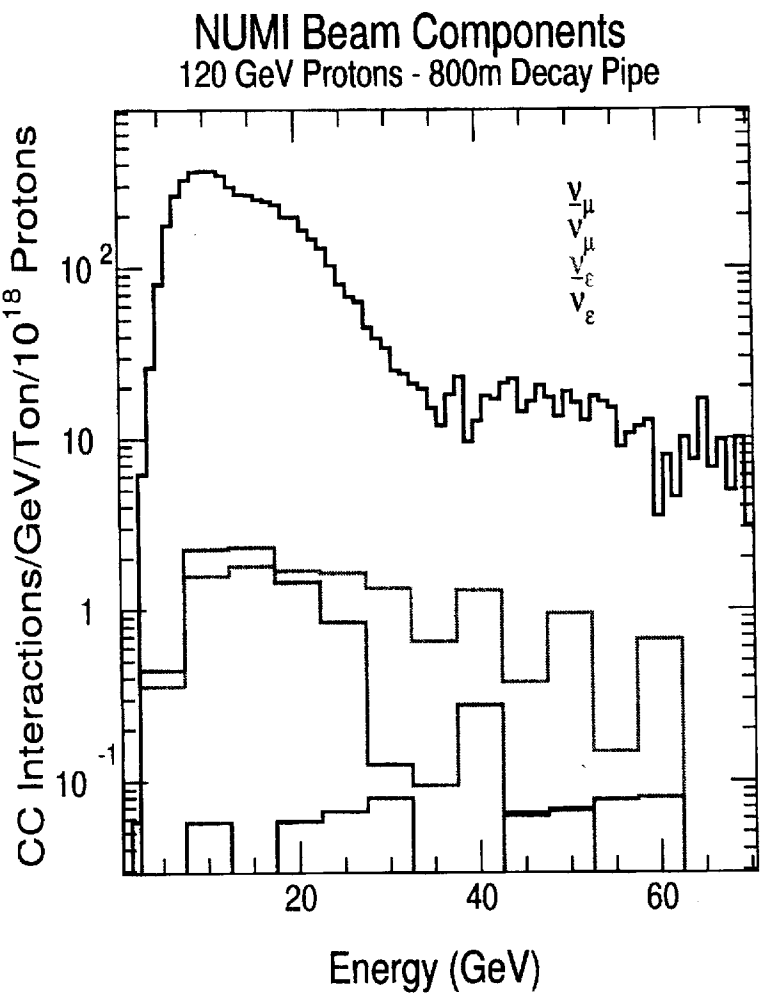

Figure 4: The simulated energy spectra for the charged-current events induced in the COSMOS detector by the ν_μ, ν_e, $\bar{\nu}_\mu$, and $\bar{\nu}_e$ components of the Main-Injector neutrino beam generated in an 800-m-long decay pipe. That the antineutrino component is small facilitates suppression of background from the decays of anticharm. Due to relatively low energy and a long decay pipe, the component of prompt τ neutrinos in the beam is negligibly small.

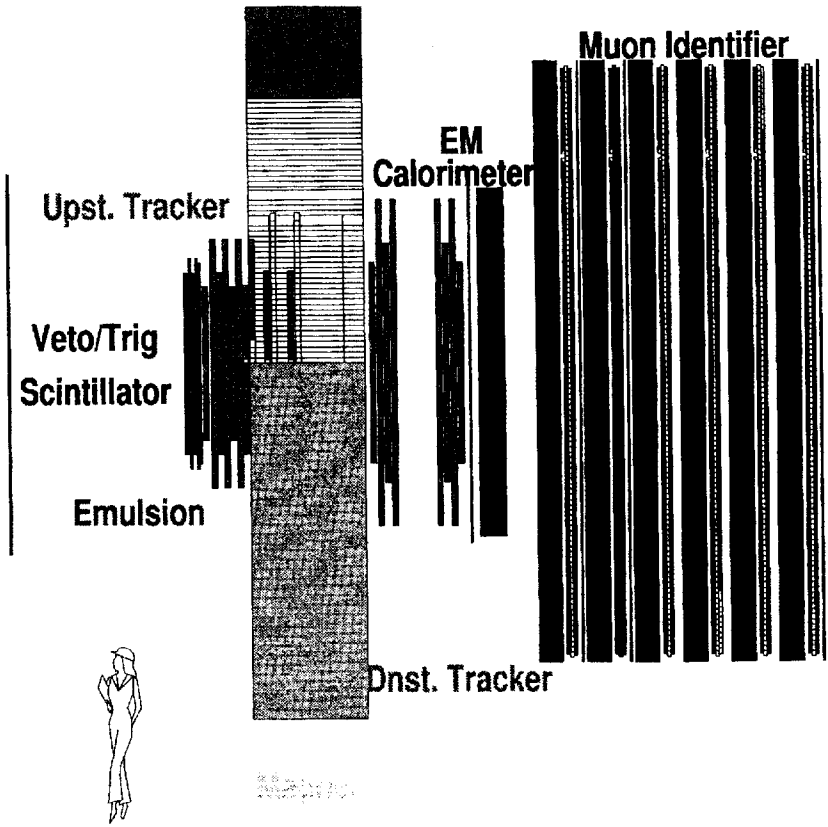

Figure 5: Elevation view of the E803/COSMOS detector.

lution in predicted track positions at the emulsion, and careful relative alighment of the large-area emulsion and tracking devices.

3. Good resolution in transverse momentum, as useful kinematic constraints use momentum vectors in the plane normal to the beam (see the previous section). The latter requires (i) good momentum resolution for charged tracks and (ii) reconstructing the energies and directions of photons from pieces, including electrons in the tracking system and splashes of energy in the electromagnetic calorimeter.

Thus, the COSMOS detector emphasizes tracking, pattern recognition, magnetic analysis, and shower reconstruction. We proceed with brief descriptions of the detector subsystems.

The emulsion target has transverse dimensions of 1.8 m by 1.4 m and contains 865 kg of Fuji emulsion with total thickness of 9.0 cm. Linking spectrometer tracks efficiently to the thick emulsion requires a complex system including interface plates and scintillating fibres, see Fig. 6. There are two identical target modules, each consisting of bulk emulsion, a scintillating-fiber tracker, and three interface plates. The fibers provide 0.5-mm two-track resolution close to emulsion, complementing the excellent pattern recognition of the multisampling drift chambers farther downstream. The interface plates, emulsion-plastic-emulsion sandwiches of 1-mm thickness, serve as verniers for pointing tracks into the bulk emulsion.

The magnet has an aperture of 2.9 by 2.3 m and delivers a p_T kick of 0.15 GeV/c. Because most photons will produce showers in thick emulsion, magnetic analysis also plays an important role in reconstructing these photons. The extended fringe field of the magnet is particularly useful for reconstructing soft shower electrons.

Most of the electronic tracking in COSMOS will rely on multisampling (jet) drift chambers that provide excellent pattern recognition, redundancy, and two-track resolution. A typical $\tau^- \to \pi^-\pi^0\nu$ event in which both photons from the π^0 have converted in emulsion is shown in Fig. 7.

It clearly illustrates the need for many pattern-recognition samples. Low-momentum tracks, mostly conversion electrons, are reconstructed and momentum-analyzed by the drift chambers upstream of and inside the magnet. The momentum resolution for particles passing through the magnet aperture in close to 2.5%.

Electromagnetic calorimetry is necessary for reconstructing the decays $\tau^- \to \pi^-(n\pi^0)\nu$ and background events. As suggested by the signature of a typical $\tau^- \to \pi^-\pi^0\nu$ event shown in Fig. 7, conversions in a 3-radiation-length emulsion target usually require the original photons to be assembled from "pieces": the tracks of conversion electrons and secondary (as well as primary) photons detected in the electromagnetic calorimeter. Therefore, the design of the electromagnetic calorimeter should emphasize good performance al low energy (down to some 100 MeV) in a high-multiplicity environment (10–20 showers per event). These requirements are fully met by the COSMOS fine-grained lead-glass calorimeter shown in 8 (in the plane normal to the beam). The square-area cells of Cherenkov lead glass with thickness of 16 radiation lengths, forming a circular assembly with radius of 1.6 m, are read out by photomultipliers. In the central area, the cells have granularity of 42.5 by 42.5 mm. Shown in Fig. 9 is the simulated π^0 signal for those $\tau^- \to \rho^-\nu$ decays in which both photons from the π^0 reached the calorimeter plane rather than converted in the target.

The downstream subsystem of the COSMOS detector is a muon identifier with thickness of 12 interaction lengths, built of 30-cm-thick slabs of iron absorber and instrumented with proportional tubes and scintillation counters. Both the positions and approximate directions

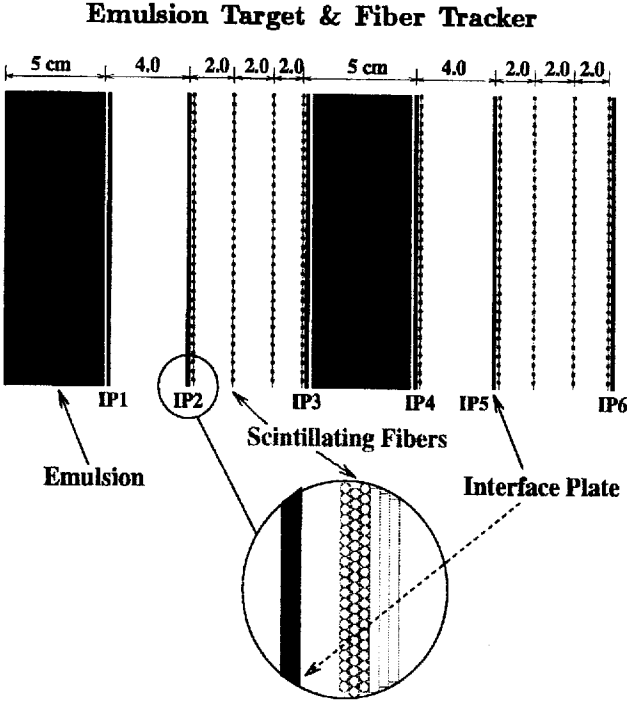

- Emulsion: 2 slabs of 1.8 m × 1.4 m × 4.5 cm, mass= 1 ton, angular resolution: $\delta\theta = \pm$ 1 mr
- Fibers: 0.5 mm dia., 7 layers/view, XY XY UV XY, Two track resolution = 0.5 mm
- Fiber readout: Image Intensifier (CCD) or VLPCs
- 6 interface layers: 2 × 100 micron thick emulsion @ 0.8 mm separation $\Rightarrow \delta\theta = \pm$ 1.3 mr

Figure 6: Schematic layout of the two bulk-emulsion targets, the six emulsion-plastic-emulsion interface plates (IP), and the 2 × 4 scintillating-fiber stations. In each of the blocks of bulk emulsion, the total thickness of emulsion is 4.5 cm and that of plastic is 0.5 cm. Each fiber station measures two orthogonal views. All dimensions are in centimeters.

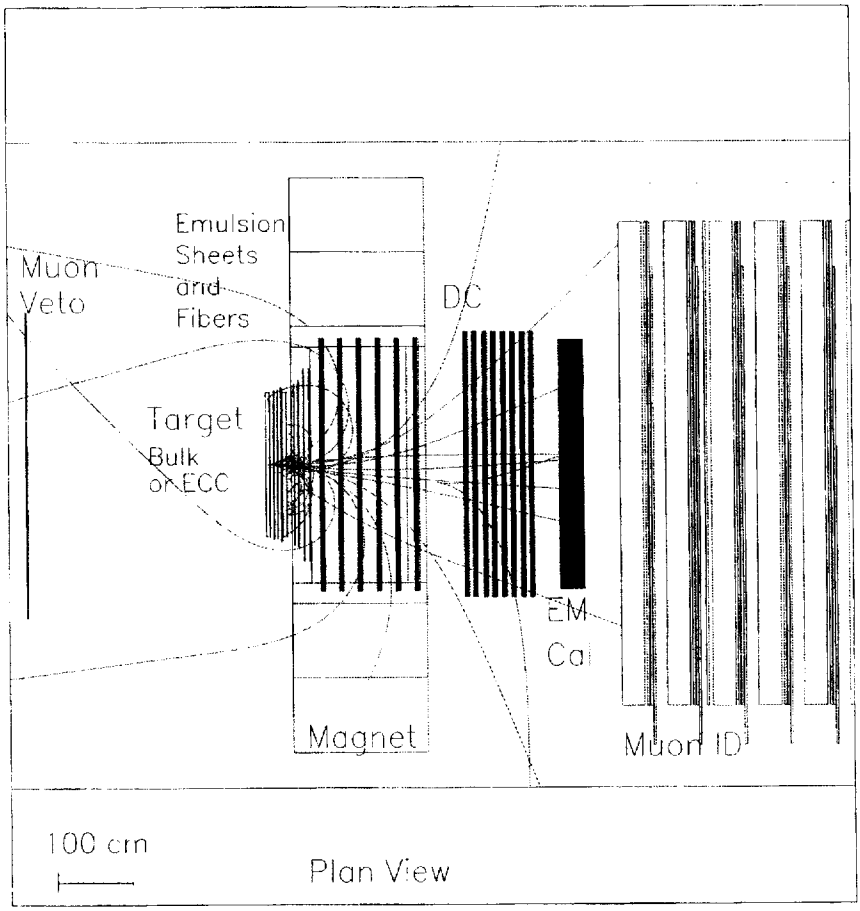

Figure 7: The combined performance of the drift-chamber tracker and the electromagnetic calorimeter in detecting a typical $\tau^- \to \pi^-\pi^0\nu$ event in which both photons from the π^0 have converted in emulsion. These photons must be reassembled from conversion electrons in the drift chambers and from secondary photons in the electromagnetic calorimeter.

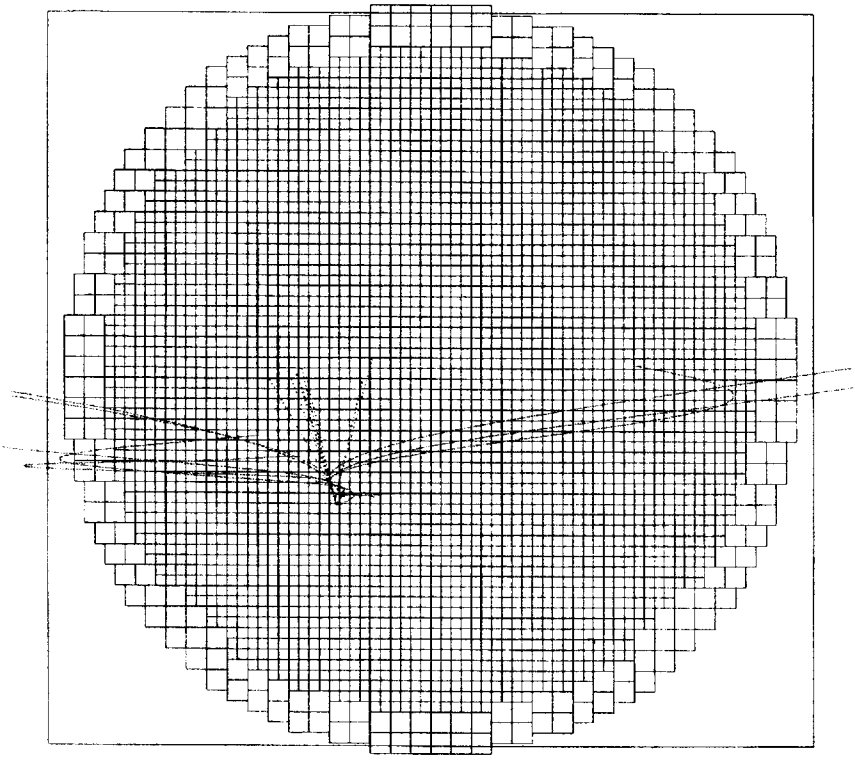

Figure 8: Schematic layout (in the plane normal to beam) of the COSMOS electromagnetic calorimeter, assembled of nearly 3000 modules of Cherenkov lead glass with thickness of 16 radiation lengths. In the central area, the cells have transverse granularity of 42.5 by 42.5 mm. Each lead-glass module is read out by a photomultiplier attached to its downstream face. Overlaid is a typical $\tau^- \to \pi^-\pi^0\nu$ decay.

of penetrating particles are measured and then matched to the momentum-analyzed tracks in the spectrometer.

4 Data Analysis

COSMOS will log on tape nearly all neutrino interactions in the emulsion target, and all recorded events will first be reconstructed offline using information from the spectrometer. Then, event vertices are located in emulsion by the scan-back method [14].

A track is suitable for scan-back if its momentum is above 1 GeV/c and its angle is within 400 mrad of the beam direction, and therefore the events featuring at least one such track are selected for extrapolating into the emulsion. Since most events have several tracks that can be used for location, event-finding efficiency is close to 100%.

The first stage of scan-back is to link a track, as reconstructed by the spectrometer and detected by the fiber tracker, to the downstream interface plate of the corresponding emulsion block. The excellent two-track separation of scintillating fibers is critical for this stage. As soon as the track is successively located in the three interface plates and then in bulk emulsion, it is followed upstream until the primary vertex is found. The candidates for one-prong decays of the τ are then found by following all primary charged tracks downstream and searching for a kink of more than 10 mrad.

As soon as a kink is found, the secondary track from the kink must be followed all the way to the exit of the emulsion and linked to the spectrometer. The kink is rejected if it reveals evidence of nuclear breakup, is positively charged, has momentum below 1 GeV/c, or has a transverse momentum of less than 0.25 GeV/c with respect to the candidate-τ direction. Next, the τ decay modes consistent with the found event must be selected. And finally, all emulsion and electronic measurements must be combined towards matching the event to one of τ decays by kinematic handles like those described in Section 2.

The scanning of several million events in emulsion on a reasonable timescale is a challenging task, and is only possible with a fully automated system [15, 16]. The emulsion plate as a whole (either an interface plate or one of the sheets of bulk emulsion) is first mounted on a movable stage with mechanical precision of 0.5 μm driven by a motor controller. Next, the plate is moved to a required position with respect to the microscope objective. The focal plane of the microscope may be tuned to select successive thin slices of the emulsion layer, sampling the dark grains with a pitch of 6 microns in depth. The optical image is digitized by a CCD camera. The digitized images for different depths are then input to a track-finding algorithm.

5 Background Processes

As the one-prong decays of charged strange particles are efficiently removed by requiring $p_T >$ 0.25 GeV with respect to candidate-τ direction, the major sources of background are (i) the admixture of prompt τ neutrinos in the beam, (ii) one-prong decays of charmed particles, and (iii) single-prong nuclear collisions of primary hadrons, occurring near the interaction vertex and showing no evidence of nuclear breakup in emulsion (the so-called white-star kinks). The estimated levels for the different sources of background are listed in Table 2.

Prompt τ neutrinos in the beam may arise from sequential tauonic decays of charmed strange mesons $D_s(1968)$ created by incident protons in the primary target: $D_s^+ \to \tau^+\nu_\tau$, $\tau^+ \to \bar{\nu}_\tau X$ (see [17] and references therein). Predicting the level of this irreducible background

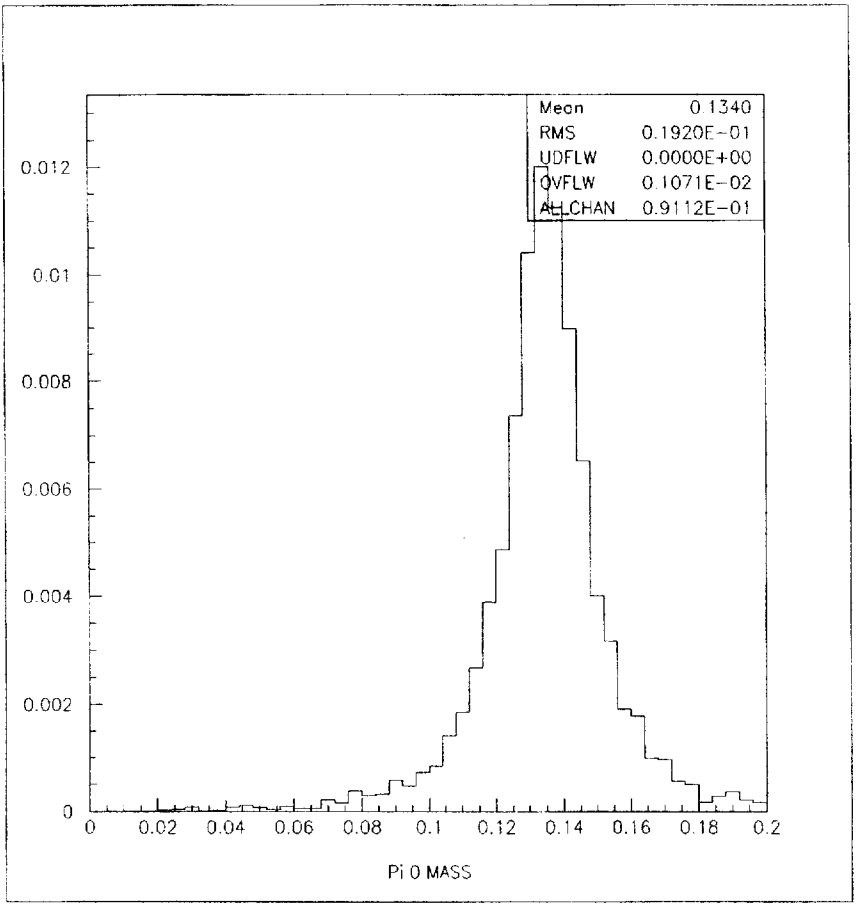

Figure 9: The simulated π^0 signal for those decays $\tau^- \to \rho^-\nu$, $\rho^- \to \pi^-\pi^0$ in which both photons from the π^0 have reached the calorimeter plane rather than converted in the target.

Source of Background	Number of Events
Decays of strange particles	< 0.04
Prompt τ neutrinos in the beam	0.2
Anticharm decays	0.6
White-star kinks	0.5
Total	1.3

Table 2: Estimated absolute backgrounds in COSMOS, assuming $8.1 \cdot 10^6$ ν_μ-induced CC interactions.

requires knowledge of the absolute cross section and of the x_F and p_T dependences for $D_s(1968)$ production in proton–nucleus collisions. That the prompt-ν_τ background is relatively low for COSMOS is due to low energy of the generic proton beam, 120 GeV, and to a large distance between the proton target and the detector (because of a large mass of the D_s^+, the ν_τ tends to be emitted at a broader angle than the ν_μ from pion and kaon decays). As the D_s cross section rapidly increases with proton energy (while the angular spread of τ neutrinos decreases), this background may pose a more serious problem for the planned high-statistics searches for $\nu_\mu \rightarrow \nu_\tau$ oscillations at CERN-SPS like [18].

The one-prong decays of charmed particles produced in CC interactions of the ν_μ will yield visible kinks on positive tracks, and therefore will be dropped. For a one-prong decay of $\bar{\nu}_\mu$-produced anticharm to mimic a τ decay, the primary μ^+ must escape identification in the muon system. In COSMOS, the number of such events is not large because the antineutrino component of the beam is small (see Section 2), and is further suppressed by rejecting those events in which a soft positive, emitted nearly back-to-back with the τ candidate in the transverse plane, penetrates one absober slab (30 cm of iron).

Like the decays of strange particles, the white-star kinks are characterized by a rapid falloff with p_T (approximately 10^{-20p_T} for $p_T > 0.1$ GeV), and therefore are largely rejected by the adopted selection of $p_T > 0.25$ GeV/c. Those occurring in CC events are rejected by the presence of a muon. The white-star kinks in NC events are additionally suppressed by scanning for a distance up to 2.5 mm downstream of the primary vertex, and by kinematic handles like the two-dimensional distributions in azimuthal angles shown in Fig. 3 (see Section 2.2).

6 Charm Production

Briefly returning to the decays of charmed particles in emulsion, we should note that apart from being a background for the τ signal, these are physically interesting in their own right. Apart from the emulsion experiment E531 [19] and a few low-statistics bubble-chamber analyses like [20], it is the dilepton studies using electronic techniques [21] that currently provide the bulk of data on charm production by neutrinos. Note however that these studies do not distinguish between various channels of charm fragmentation (D, D^*, D_s, D_s^*, Λ_c, *etc.*) and have to rely on model predictions in deriving the cross section of charm production. With a charm rate of roughly one per 100 CC events, COSMOS may collect a sample of charm decays comparable to those of current photoproduction and hadroproduction experiments [22]. This sample will allow precise determinations of the CKM matrix element V_{cd} and of the c-quark mass, and will provide an insight into the dynamics of charm production by neutrinos.

7 Contribution to COSMOS of the Institute of Theoretical and Experimental Physics, Moscow

As a member of the E803/COSMOS Collaboration, ITEP actively contributes to either constructing the detector and developing the methods for data analysis.

7.1 Constructing the COSMOS Detector

On the level of detector hardware, the major respronsibility of ITEP is the electromagnetic calorimeter. Of the three calorimeter options based on different techniques, the ITEP design of a fine-grained circular assembly of lead-glass Cherenkov modules (see Fig. 8) showed superior resolution in energy and position of electromagnetic showers and the best suppression of neutron background, and therefore was selected for construction. ITEP has already delivered to Fermilab a major part of the required lead-glass blocks and photomultipliers, and currently participates in calibrating the multicell prototypes of the electromagnetic calorimeter.

ITEP is also involved in designing and manufacturing the spectrometer magnet and the muon system.

7.2 Generating the ν_μ-Induced Events

In the COSMOS experiment that aims at extracting the τ signal from a formidable sample of nearly 10^7 neutrino events, ν_μ collisions with the nuclei of emulsion must be understood in full detail. The problems with a purely theoretical description of neutrino-emulsion collisions are twofold:

- at energies below 50 GeV, one may well overstretch the limits of perturbative QCD: with the Main-Injector neutrino beam (see Fig. 4), almost a half of all deep-inelastic events are expected to have Q^2 below 4 GeV^2. In the parton-model language, at neutrino energy on the order of 10–20 GeV the wavelength of the momentum transfer may prove too large for incoherently probing a single parton (which is then expected to hadronize into visible particles);

- nuclear effects in neutrino collisions with heavy nuclei cannot be reliably taken into account.

An alternative approach to simulating neutrino collisions, as proposed and implemented by the ITEP group, is to rely on "live" neutrino events detected in bubble-chamber experiments. (ITEP has a large bank of neutrino data from bubble-chamber experiments carried out at Fermilab, CERN, and IHEP Protvino.) The ITEP generator of neutrino events is based on the heavy-freon data from the bubble chamber SKAT at IHEP Protvino [23] ($\langle E_{CC} \rangle = 10.3$ GeV) and on the neon data from BEBC at CERN [24] ($\langle E_{CC} \rangle = 53$ GeV). The advantages of the SKAT–freon data are that (i) the muons are efficiently identified down to 500 MeV/c, (ii) in CC events the undetected particles account for only some 4a heavy-freon target (CF_3Br) should be similar to those in emulsion. For the CC events, the strategy is to generate E_ν according to the required spectrum (see Fig. 4 and then to select the nearest live event. As the mean neutrino energy of COSMOS falls between those for the SKAT–freon and BEBC–neon data, one will thereby largely select SKAT events at low energy and BEBC events at high energy where the effects of the BEBC selection $p_\mu > 4$ GeV are less devastating. The NC events are simulated by simply dropping muons in thus selected CC events.

7.3 Simulating τ Events in the Detector

Relying on its own code for generating the events of τ production and decay and using the GEANT package, the ITEP group has started extensive simulations of the detector response to the τ signal. These simulations, that are still at an early stage, are aimed at detailing the procedures for reconstructing the leptonic and semileptonic decays of the τ and at estimating the experimental acceptances.

8 Summary

COSMOS is a ν_τ appearance experiment sensitive to very small neutrino-mixing angles and to neutrino mass differences in the cosmologically interesting region. The emphasis is made on the discovery potential: the experiment is designed to demonstrate an unambiguous τ signal, should the $\nu_\mu \to \nu_\tau$ transition exist with a probability that is at least five times larger than the upper limit for a null hypothesis, $P < 1.4 \times 10^{-5}$ at 90% confidence level. By analyzing the decays of charmed particles produced by neutrinos, COSMOS will also provide precise determinations of the CKM matrix element V_{cd} and of the c-quark mass. The hybrid detector combines a massive emulsion target and an electronic spectrometer, and will be exposed to a wide-band neutrino beam of Main Injector at Fermilab.

References

[1] B. Pontecorvo, Sov. Phys. JETP 6, 429 (1958); Z. Maki *et al.*, Progr. Theor. Phys. 28, 870 (1962)

[2] T. Kirsten, GALLEX Coll., Proc. Neutrino-96 (Helsinki, 1996), in press; V. N. Gavrin, SAGE Coll., *ibid.*; K. Lande, Homestake Coll., *ibid.*; Y. Suzuki, Kamiokande Coll., *ibid.*

[3] L. Wolfenstein, Phys. Rev. D17, 2369 (1978); D20, 2634 (1979); S. Mikheev and A. Smirnov, Yad. Fiz. 42, 1441 (1985)

[4] D. Caspers *et al.*, IMB Coll., Phys. Rev. Lett. 66, 2561 (1991); K. S. Hirata *et al.*, Kamiokande Coll., Phys. Lett. B280, 146 (1992); Y. Fukuda *et al.*, Kamiokande Coll., Phys. Lett. B335, 237 (1994)

[5] C. Athanassopoulos *et al.*, LSND Coll., preprint LA-UR-96-1326 (1996)

[6] M. Gell-Mann, P. Ramond, and R. Slansky, in *Supergravity*, eds. P. van Nieuwenhuizen and D. Freedman (North Holland, Amsterdam, 1979), p. 315

[7] N. Ushida *et al.*, E531 Coll., Phys. Rev. Lett. 57, 2897 (1986)

[8] M. de Jong *et al.*, CHORUS Coll., preprint CERN-PPE/93-131 (1993); E. Eskut *et al.*, CHORUS Coll., preprint CERN-PPE/97-33 (1997)

[9] K. Kodama *et al.*, E803/COSMOS Coll., Fermilab Proposal P803 (1993)

[10] K. Kodama *et al.*, Update Report on Fermilab E803/COSMOS, Fermilab, 1995

[11] E. Ables *et al.*, MINOS Coll., Fermilab Proposal P875 (1995)

[12] K. Kodama *et al.*, E653 Coll., preprint DPNU-96-33, June 1996

[13] F. Abe *et al.*, Phys. Rev. Lett. 75, 11 (1995)

[14] S. Aoki *et al.*, Nucl. Instruments and Methods B51, 446 (1990)

[15] T. Nakano, Ph. D. Thesis, University of Nagoya (1997)

[16] G. Rosa *et al.*, preprint Univ. Salerno DSF US 97/1 (1997), submitted to Nucl. Instruments and Methods

[17] M.C. Gonzales-Garcia and J.J. Gomez-Cadenas, Phys. Rev. D55, 1297 (1997)

[18] A.S. Ayan *et al.*, TOSCA Coll., Letter of Intent, CERN-SPSC/97-5, SPSC/I213 (March 14, 1997)

[19] N. Ushida *et al.*, E531 Coll., Phys. Lett. 121B, 292 (1983)

[20] A. Asratyan *et al.*, Big Bubble Chamber Neutrino Coll., Z. Phys. C68, 43 (1995)

[21] A. Rabinovitz *et al.*, CCFR Coll., Phys. Rev. Lett. 70, 134 (1993)

[22] E.M. Aitala *et al.*, E791 Coll., Phys. Lett. B371, 157 (1996); P.L. Frabetti *et al.*, E687 Coll., Phys. Lett. B351, 591 (1995)

[23] V.V. Ammosov *et al.*, SKAT Coll., Z. Phys. C42, 361 (1989); C41, 527 (1989); C40, 493 (1988); C40, 487 (1988)

[24] K. Varvell *et al.*, WA59 Coll., Z. Phys. C36, 1 (1987)

А.Асратян, М.Балац, Г.Давиденко и др.

Поиски нейтринных осцилляций в эксперименте КОСМОС в Фермилаб

Подписано к печати 27.08.98 Формат 60x90 I/I6
Усл.-печ.л.I,25. Уч.изд.л.-0,9. Тираж I2I экз. Заказ 30.
Индекс 3649

Отпечатано в ИТЭФ, II7259,Москва, Б.Черемушкинская, 25

Индекс 3649

Препринт 30-98, ИТЭФ, 1998